Results in Physics 52 (2023) 106753

Contents lists available at ScienceDirect

Results in Physics

journal homepage: www.elsevier.com/locate/rinp

An efficient method for the fractional electric circuits based on Fibonacci wavelet

Shahid Ahmed [a], Kamal Shah [b], Shah Jahan [a,*], Thabet Abdeljawad [b,c,d,e,*]

[a] Department of Mathematics, Central University of Haryana, Mahendergarh 123029, India
[b] Department of Mathematics and Sciences, Prince Sultan University, Riyadh 11586, Saudi Arabia
[c] Department of Medical Research, China Medical University, Taichung 40402, Taiwan
[d] Department of Mathematics Kyung Hee University,26 Kyungheedae-ro, Dongdaemun-gu, Seoul 02447, Republic of Korea
[e] Department of Mathematics and Applied Mathematics, School of Science and Technology, Sefako Makgatho Health Sciences University, Ga-Rankuwa, South Africa

ARTICLE INFO

MSC:
26A33
65D15
65T60
97M50

Keywords:
Fractional calculus
Caputo fractional derivatives
Fibonacci wavelets
Numerical methods
Electrical circuits

ABSTRACT

In this article, we provide effective computational algorithms based on Fibonacci wavelet (FW) to approximate the solution of fractional order electrical circuits (ECs). The proposed computational algorithm is novel and has not been previously utilized for solving ECs problems. Firstly, we have constructed the operational matrices of fractional integration (OMFI). Secondly, we transform the given initial value problems into algebraic equations, we used the Riemann–Liouville (R–L) fractional integral operator. The proposed approach is capable of handling a wide range of fractional order dynamics in ECs. To validate the effectiveness of the method, four models of electrical circuits with fractional order parameter are considered. The numerical results are compared with exact solutions and absolute errors are calculated to demonstrate the accuracy and efficiency of the approach. The proposed method provides a valuable tool for analyzing and designing fractional order systems in electrical engineering, offering improved accuracy and capturing the intricate behavior of complex systems.

Introduction

Fractional calculus is an extension of classical calculus, originally developed by Newton and Leibnitz. Over the past two decades, various aspects of fractional calculus have gained significant attention, leading to a growing interest among researchers in this field. Particularly, the applications of fractional calculus, especially in simulating physical problems, have become increasingly popular. There are several approaches for generating fractional order derivatives, including Caputo, Riemann–Liouville(RL), Baleno fractional, Grünwald–Letnikov. Among these methods, Caputo's approach stands out due to its ability to handle initial conditions defined in terms of field coordinates and their integer order. To maintain clarity and avoid confusion, we will use fractional derivatives (FDs) in the sense of Caputo throughout the remainder of this article. Some applications of fractional derivatives are found in [1, 2]. Also fractional differential equation with biological application [3] and water borne disease [4]. For further studies on fractional operators we refer [1,2,5–7].

Definition 1 ([1]). The RL fractional operator of order $\alpha > 0$ for the function $\theta(\ell)$ is defined as:

$$\xi^{\alpha}\theta(\ell) = \frac{1}{\Gamma(\alpha)} \int_0^{\ell} \frac{\theta(\tau)}{(\ell-\tau)^{1-\alpha}}\, d\theta, \quad \ell > 0,$$

where the gamma function $\Gamma(.)$ is involved, some properties of the operator ξ^{α} are: $\xi^{\alpha}\xi^{\beta}g(\ell) = \xi^{\alpha+\beta}g(\ell), \quad \alpha, \beta > 0$, and

$$\xi^{\alpha}\ell^{\beta} = \frac{\Gamma(1+\beta)}{\Gamma(1+\alpha+\beta)}\ell^{\alpha+\beta}, \quad \beta > -1.$$

Definition 2 ([1]). The definition of the Caputo derivative D^{α} for the function $\theta(\ell)$ is as follows:

$$D^{\alpha}\theta(\ell) = \frac{1}{\Gamma(n-\alpha)} \int_0^{\ell} \frac{\theta^{n}(\tau)}{(\ell-\tau)^{\alpha-n+1}}\, d\tau, \quad n-1 < \alpha \le n, n \in \mathbb{N},$$

* Corresponding authors.
E-mail addresses: Shahjahan@cuh.ac.in (S. Jahan), tabdeljawad@psu.edu.sa (T. Abdeljawad).

https://doi.org/10.1016/j.rinp.2023.106753
Received 14 June 2023; Received in revised form 12 July 2023; Accepted 12 July 2023
Available online 20 July 2023

below are some properties of D^{α}

$$D^{\alpha}\ell^{\beta} = \frac{\Gamma(1+\beta)}{\Gamma(1+\beta-\alpha)}\,\ell^{\beta-\alpha}, \quad 0 < \alpha < \beta+1,\ \beta > -1;$$

$$\xi^{\alpha} D^{\alpha}\theta(\ell) = \theta(\ell) - \sum_{k=0}^{n-1} f^{k}(0^{+})\,\frac{\ell^{k}}{k!}, \quad n-1 < \alpha \le n, n \in \mathbb{N};$$

$$D^{\alpha}C = 0, \quad C \text{ is a constant.}$$

The derivative and integral operators of fractional order have gained significant attention due to their valuable properties. These properties include non-locality, memory, and a higher degree of freedom compared to classical derivative and integral operators. These useful properties make it possible to create more precise and sensitive models of important systems in engineering and science [1,5]. In recent years, many new models have been created using fractional operators including simulation of fractional differential equation using numerical Laplace transform [2,6], electrical applications [8], fractal–fractional tobacco models [9], nonlinear pantograph equations [10]. However, it is important to acknowledge that the main challenge in working with fractional models lies in obtaining their analytic solutions, which often becomes a difficult task. Consequently, researchers have predominantly focused on exploring approximation methods for addressing such problems. In recent years, interest in fractional order dynamics in electrical circuits has grown as a potential area of study. This is because it allows for detailed modeling and analysis of complex processes that standard integer-order models cannot effectively represent. Several papers have discussed the solution of fractional ECs using various mathematical methods. Arora et al. [11] applied the Legendre wavelet method, while Atangana et al. [7] studied the ECs model using a FDs without a singular kernel. Gómez et al. [6] employed the Caputo derivative and Laplace transform to solve $\mathcal{RLC}$ ECs. Shah et al. [12] addressed $\mathcal{RL}$ ECs by utilizing the Laplace transform of the FDs in the Caputo sense. Gill et al. [13] obtained solutions for the $\mathcal{RLC}$ circuit by utilizing the Sumudu transform and expressing them in terms of the Mittag-Leffler function. Alsaedi et al. [14] explored fractional ECs equations using different fractional definitions. Furthermore, Gómez et al. [15] focused on analytical and numerical solutions for ECs described by FDs. More recently, Sene et al. [16] derived analytical solutions for ECs while considering certain generalized FDs. Wavelet-based numerical methods have found applications in various areas, including signal and image processing, data compression, scientific computing, and solving lumped and distributed parameter system [17], also solving differential and integral equations [18,19]. They offer advantages over traditional methods by allowing for adaptive and multiscale analysis, which can capture both global and local features of the problem. These approaches have been carefully examined and applied in a wide range of scientific and engineering fields, offering a powerful and flexible framework for numerical analysis and computation. Wavelets are widely employed in finding numerical solutions for various differential and integral equations. In recent years, wavelet techniques have been widely employed by researchers to solve fractional-order differential equations. Various types of wavelets have been explored in the literature, including Haar wavelets [17,20], Legendre wavelets [11], Fibonacci wavelets,[21,22] and Gegenbaur wavelets [19]. The Fibonacci polynomials has gained significant attention due to its superior characteristics compared to Legendre polynomials. The FW consist of fewer terms as compared to other polynomial wavelets which accelerates computation and reduces the chances of errors occurring. As a result, numerous studies have been conducted on Fibonacci wavelets. The key features of the Fibonacci wavelet method (FWM) are as follows:

- The FW is a function that can be defined at various scales and has a wide range of uses because of its characteristics, including compact support and vanishing moments.
- FWM is effective when analyzing solutions that involve discontinuities and abrupt changes. To apply this technique to understanding a function, we first create a window for it at the point of discontinuity and sharp edge.
- This approach does not appear to have any significant weaknesses. However, this approach only works in a limited domain, not a broad one. We require the employment of transformations to operate throughout the wide domain.

This polynomial based wavelet method has been used to resolve the Fredholm integral equation [18], fractional order logistic growth model [21], Bagley-Torvik equation [22]. It is evident that Fibonacci wavelets are well-suited for approximating smooth and piecewise smooth functions. Despite the increasing interest in this field, the number of articles specifically focusing on dynamics of ECs remains relatively limited. One recent development by Altaf et al. [23] involves the utilization of the Haar wavelet for solving fractional ECs. Chouhan [24] solved the fractional $\mathcal{RL}$ circuit by utilizing Legendre multiwavelet. Recently Adel et al. [25] numerically discussed the analysis and simulation of electric $\mathcal{RL}$ circuit. Fibonacci wavelets produced by Fibonacci polynomials are a new addition to the field of wavelet families. It has added an advantage in contrast with the other wavelet methods [26]. The Fibonacci polynomials, typically have fewer terms compared to the Legendre polynomials. This disparity in the number of terms can contribute to reduced CPU time during computations [27,28]. Error components in the operational matrix of integration representing Fibonacci polynomials are less than those of Legendre polynomials [29,30]. Using the Mathematica command Fibonacci [m,x], the coefficient of the Fibonacci polynomials can be easily obtained in computer programmes. Motivated with the nice properties and advantages of FW over the other wavelet methods, we have solved fractional electric circuit models. We use Caputo fractional derivatives and Fibonacci wavelet-based methods to understand and analyze fractional order dynamics in ECs. In this paper, we consider the fractional order models of ECs because they enhance the understanding of complex electrical systems, improve modeling accuracy, enable control strategies, and stimulate innovation in electrical engineering. The behavior of electrical circuits cannot be accurately described by traditional integer-order models. By addressing these topics, the study independently has implications for circuit design, control strategies, and the broader field of fractional calculus. The proposed approach offers a comprehensive framework for accurately modeling and analyzing the behavior of circuit variables, such as currents and voltages, while considering the fractional order dynamics of the system. Considering the importance of fractional ECs in modern technology, which are crucial for designing various complex systems such as signals systems, mechanical, dynamical, aerospace, industrial, control, computer, communication, and electronic, as well as consumer products, it becomes essential to have a solid understanding of the mathematical model that describes them as fractional differential models, such as electrical circuit of non integer order via fractional derivatives [31]. In [32], a new collection of real world applications of fractional calculus in science and engineering is given. Analytical solution for the electric circuit model in fractional order is studied in [12,22]. By studying these models, one can gain a deeper insight into the behavior of different types of linear time ECs.

The remaining sections of the paper will be discussed as: In Section “Formulation of fractional order models” contains the formulation of fractional order models. Section “Fibonacci wavelet” provides a brief about FW and its function approximation. In Section “OMFI of Fibonacci wavelets”, the operational matrix of fractional order using the FW and the block pulse functions (BPF) are examined. Section “Error estimation and numerical results” focuses on error analysis and numerical problems, showcasing the efficiency and precision of the proposed approach. Finally, a concise conclusion is presented.

Formulation of fractional order models

Here, we will present the construction of models for conventional electrical $\mathcal{RC}, \mathcal{RL}, \mathcal{LC}$, and $\mathcal{RLC}$ circuits. To derive the corresponding

fractional forms of each model using a series of straightforward steps guided by the following principles: *Ohm's law:* The voltage drop across a resistor, denoted as $\mathcal{VR}$, is directly proportional to the current passing through it, represented as $q(\ell)$. The constant of proportionality is the resistance $\mathcal{R}$, measured in Ohm's. Therefore, the voltage drop across a resistor can be calculated as $\mathcal{VR} = \mathcal{R}J$. *Law of inductance:* The principle of inductance states that through empirical observations, a connection has been established between the voltage decrease across an inductor and the instantaneous rate of change of the electric current, denoted as $q(\ell)$. This relationship is expressed mathematically as $\Delta\mathcal{V} = \mathcal{L}(\frac{dq}{d\ell})$, where $\Delta\mathcal{V}$ represents the voltage drop across the inductor, $\mathcal{L}$ denotes the inductance (a constant of proportionality), and $(\frac{dq}{d\ell})$ represents the instantaneous rate of change of the electric current.
Kirchhoff's voltage law in a closed loop: The total voltage supplied $\mathcal{V}_E$ is equal to the sum of voltage drops across the other components in the loop.

There are two main laws:

- Kirchhoff's Current Law (KCL): KCL states that the sum of currents entering a node (or junction) in an electrical circuit is equal to the sum of currents leaving that node.
- Kirchhoff's Voltage Law (KVL): KVL states that the sum of voltage drops (or potential differences) around any closed loop in a circuit is equal to zero.
- Kirchhoff's laws are used to analyze and solve complex electrical circuits by writing and solving a set of simultaneous equations based on the laws.

Fractional $\mathcal{LC}$ circuit model: An $\mathcal{LC}$ circuit, is a simple ECs consisting of an inductor $\mathcal{L}$ and a capacitor $\mathcal{C}$ connected in parallel or series. The $\mathcal{LC}$ circuit has several important characteristics such as resonance, energy storage, oscillations. To derive the fractional $\mathcal{LC}$ circuit, we start with the classical differential equation for an $\mathcal{LC}$ circuit as:

$$\frac{dq(\ell)}{d\ell} + \frac{1}{\mathcal{LC}}q(\ell) = \frac{F}{\mathcal{L}}. \tag{1}$$

To obtain the fractional version, applying the FDs operator of order α to Eq. (1), involving fractional inductor $\mathcal{L}$ and fractional capacitor $\mathcal{C}$ we have:

$$D^{\alpha}\left(\frac{dq(\ell)}{d\ell}\right) + \frac{1}{\mathcal{LC}}q(\ell) = \frac{F}{\mathcal{L}}. \tag{2}$$

Simplifying further, we obtain the fractional $\mathcal{LC}$ circuit equation in the form:

$$D^{\alpha}[q(\ell)] + \zeta^2 q(\ell) = \mathcal{E}(\ell), \tag{3}$$

where $\zeta^2 = \frac{1}{\mathcal{LC}}$, and $\mathcal{E}(\ell) = \frac{F}{\mathcal{L}}$. This Eq. (3) represents the fractional $\mathcal{LC}$ circuit, where $\mathcal{L}$ is the inductance, $\mathcal{C}$ is the capacitance, F is electomotive force, $q(\ell)$ is the charge, $\mathcal{E}(\ell)$ is the external input, and D^{α} denotes the FDs of order α.

Fractional $\mathcal{RC}$ circuit model: In an $\mathcal{RC}$ circuit, the voltage drop across a capacitor with capacitance $\mathcal{C}$ is given by $\frac{1}{\mathcal{C}}q(\ell)$. Therefore, applying the second law of Kirchhoff's, we obtain:

$$\mathcal{R}J(\ell) + \frac{1}{\mathcal{C}}q(\ell) = \mathcal{E}(\ell). \tag{4}$$

Since $J(\ell)$ and $q(\ell)$ are related by $J(\ell) = \frac{dq(\ell)}{d\ell}$, so Eq. (4) can be rewritten as:

$$\mathcal{R}\frac{dq(\ell)}{d\ell} + \frac{1}{\mathcal{C}}q(\ell) = \mathcal{E}(\ell).$$

The equation can be represented in its fractional form as:

$$\mathcal{R}D^{\alpha}q(\ell) + \frac{1}{\mathcal{C}}q(\ell) = \mathcal{E}(\ell), \quad \ell \in [0,1], 0 < \alpha \leq 1, \tag{5}$$

with initial condition (IC) $q(0) = q_0$ Fractional order $\mathcal{RC}$ circuits have gained attention in recent years due to their ability to model and represent certain complex systems more accurately. They have been used in various applications such as signal processing, control systems, and biomedical engineering.

Fractional $\mathcal{RL}$ circuit model: The classical $\mathcal{RL}$ model refers to a circuit model that includes a resistor $\mathcal{R}$ and an inductor $\mathcal{L}$ as its main components. By applying Kirchhoff's law and consider $\mathcal{E} = \mathcal{V}_r + \mathcal{V}_l$. The mathematical representation of the model is expressed through a differential equation as:

$$\mathcal{L}\frac{dq(\ell)}{d\ell} + \mathcal{R}q(\ell) = \mathcal{E}(\ell), \quad q(0) = q_0, \quad \ell \in [0,1]. \tag{6}$$

By incorporating the resistance $\mathcal{R}$ and inductance $\mathcal{L}$ into the circuit configuration, either in series or in parallel, the differential equation for an electrical circuit can be expressed in the fractional-order (Liouville–Caputo sense) for $0 < \alpha \leq 1$. The Eq. (6) will adopt the form:

$$\mathcal{L}D^{\alpha}q(\ell) + \mathcal{R}q(\ell) = \mathcal{E}(\ell), \quad \ell \in [0,1], \quad 0 < \alpha \leq 1, \tag{7}$$

with IC $q(0) = q_0$.

Fractional $\mathcal{RLC}$ circuit model: In accordance with Kirchhoff's law, the applied voltage $\mathcal{E}(\ell)$ within a closed loop should be equivalent to the total sum of voltage drops across the components of the $\mathcal{RLC}$ circuit. Additionally, it is known that the current $J(\ell)$ is related to charge $q(\ell)$ on capacitor through a relationship:

$$J(\ell) = \frac{dq(\ell)}{d\ell},$$

so by summing the three voltage drops $\mathcal{L}\frac{dJ(\ell)}{d\ell} = \mathcal{L}\frac{d^2q(\ell)}{d\ell^2}$, $J(\ell)\mathcal{R} = \mathcal{R}\frac{dq(\ell)}{d\ell}$, $\frac{1}{\mathcal{C}}q(\ell)$. By adding the sum of the voltage drops across the components of the $\mathcal{RLC}$ circuit and equating it to the impressed voltage, we derive second-order differential equation as:

$$\mathcal{L}\frac{d^2q}{d\ell^2} + \mathcal{R}\frac{dq}{d\ell} + \frac{1}{\mathcal{C}}q(\ell) = \mathcal{E}(\ell). \tag{8}$$

The fractional version of the equation will take the form:

$$\mathcal{L}D^{\lambda}q(\ell) + \mathcal{R}D^{\delta}q(\ell) + \frac{1}{\mathcal{C}}q(\ell) = \mathcal{E}(\ell), \quad \ell \in [0,1],$$
$$0 < \delta \leq 1, \text{ and } 1 < \alpha \leq 2, \tag{9}$$

with $q(0) = q_0$ and $q'(0) = q_1$.

We have, if $\lambda = 2$ and $\delta = 1$, Eq. (9) becomes the classical equation for $\mathcal{RLC}$ circuit. A classical $\mathcal{RLC}$ circuit, also known as a series $\mathcal{RLC}$ circuit is a basic electrical circuit that consists of a resistor ($\mathcal{R}$), an inductor ($\mathcal{L}$), and a capacitor ($\mathcal{C}$) connected in series. It is a fundamental circuit configuration used to study the behavior of electrical components and systems. The $\mathcal{RLC}$ circuit can exhibit different characteristics based on these factors, including resonance, damping, and frequency-dependent impedance. Analysis and design of $\mathcal{RLC}$ circuits involve techniques such as Kirchhoff's laws, differential equations, complex impedance, and transfer functions.

Fibonacci wavelet

The FW offers distinct characteristics that contribute to its utility in various signal processing and analysis applications. It demonstrates self-similarity, enabling it to retain its shape when scaled or translated to different positions. This allows for the analysis of signals at different scales or resolutions. The FW also has good localization properties, that is concentrated in both time and frequency domains. The FW is a type of wavelet function that is derived from the Fibonacci sequence or polynomials, a series of numbers in which each number is the sum of the two preceding numbers (e.g., 0, 1, 1, 2, 3, 5, 8, 13, and so on). The recurrence relation defines the Fibonacci polynomials for any positive real number $\ell \in \mathbb{R}^+$,

$$Q_{m+2}(\ell) = \ell Q_{m+1}(\ell) + Q_m(\ell) \quad (m \geq 0). \tag{10}$$

The Fibonacci polynomials, which satisfy the initial conditions $Q_0(\ell) = 0$ and $Q_1(\ell) = 1$ [33], can also be represented using a general formula

$$Q_m(\ell) = \begin{cases} 0, & \text{if } m = 0, \\ 1, & \text{if } m = 1, \\ \ell Q_{m-1}(\ell) + Q_{m-2}(\ell), & \text{if } m > 1, \end{cases} \tag{11}$$

and the closed-form is

$$Q_{m-1}(\ell) = \frac{\alpha^m - \beta^m}{\alpha - \beta} \quad (m \geq 1).$$

The roots of polynomial $x^2 - \ell x - 1$ associated with the recursion are denoted by α and β. Additionally, the Fibonacci polynomials can be represented in a power-form as:

$$Q_m(\ell) = \sum_{i=0}^{\lfloor m/2 \rfloor} \binom{m-i}{i} \ell^{m-2i} \quad (m \geq 0). \tag{12}$$

The notation $\lfloor \cdot \rfloor$ represents the commonly known floor function. Alternatively the Fibonacci polynomials $Q_m(\ell)$ are represented in matrix form as:

$$Q(\ell) = PL(\ell), \tag{13}$$

where the equation

$$Q(\ell) = \begin{pmatrix} Q_0(\ell) \\ Q_1(\ell) \\ Q_2(\ell) \\ \vdots \end{pmatrix} \quad L(\ell) = \begin{pmatrix} 1 \\ \ell \\ \ell^2 \\ \ell^3 \\ \vdots \end{pmatrix} \quad \text{and}$$

$$P = \begin{pmatrix} 1 & 0 & 0 & 0 & 0 & 0 & 0 & \dots \\ 0 & 1 & 0 & 0 & 0 & 0 & 0 & \dots \\ 1 & 0 & 1 & 0 & 0 & 0 & 0 & \dots \\ 0 & 2 & 0 & 1 & 0 & 0 & 0 & \dots \\ 1 & 0 & 3 & 0 & 1 & 0 & 0 & \dots \\ 0 & 3 & 0 & 4 & 0 & 1 & 0 & \dots \\ 1 & 0 & 6 & 0 & 5 & 0 & 1 & \dots \\ \vdots & \vdots & \vdots & \vdots & \vdots & \vdots & \vdots & \ddots \end{pmatrix}.$$

The Fibonacci polynomials have the following notable properties:

$$\int_0^{\ell} Q_m(s)\, ds = \frac{1}{m+1} \left[Q_{m+1}(\ell) + Q_{m-1}(\ell) - Q_{m+1}(0) - Q_{m-1}(0) \right], \tag{14}$$

$$\int_0^1 Q_m(\ell) Q_n(\ell)\, d\ell = \sum_{i=0}^{\lfloor m/2 \rfloor} \sum_{j=0}^{\lfloor n/2 \rfloor} \binom{m-i}{i} \binom{m-j}{j} \frac{1}{m+n-2i-2j+1}. \tag{15}$$

The Fibonacci wavelets represent a unique set of compactly-supported wavelets that are derived from the Fibonacci polynomials and defined on $[0, 1]$ as follows:

$$\Psi_{n,m}(\ell) = \begin{cases} \frac{2^{(k-1)/2}}{w_m^{1/2}} Q_m\left(2^{k-1}\ell - n + 1\right) & \text{if } \frac{n-1}{2^{k-1}} \leq \ell < \frac{n}{2^{k-1}}, \\ 0 & \text{otherwise}, \end{cases} \tag{16}$$

where $Q_m(\ell)$ represents the Fibonacci polynomial of degree m defined in Eq. (12), while k and n correspond to the level of resolution, with k taking values from $\mathbb{Z}^+$ and n representing the translation parameter, ranging from 1 to 2^{k-1}. The coefficient $w_m^{1/2}$ in Eq. (16) serves as a normalization factor and calculated using Eq. (15) as:

$$w_m = \int_0^1 (Q_m(\ell))^2 d\ell, \quad m = 0, 1, \dots, M-1.$$

The FW (16) can be represented as:

$$\Psi_{n,m}(\ell) = \frac{2^{(k-1)/2}}{w_m^{1/2}} Q_m\left(2^{k-1}\ell - n + 1\right) \chi_{I_{n,k}}(\ell), \tag{17}$$

The characteristic function $\chi_{I_{n,k}}(\ell)$ is defined on the interval $\frac{n-1}{2^{k-1}} \leq \ell < \frac{n}{2^{k-1}}$. When selecting $k = 2$ and $M = 3$, we obtain the following set of FW:

$$\left.\begin{aligned} &\Psi_{1,0}(\ell) = \sqrt{2}, \\ &\Psi_{1,1}(\ell) = 2\sqrt{6}\ell, \\ &\Psi_{1,2}(\ell) = \sqrt{\tfrac{15}{14}}\left(1 + 4\ell^2\right), \\ &\Psi_{1,3}(\ell) = \sqrt{\tfrac{960}{38}}\left(2\ell^3 + \ell\right), \end{aligned}\right\} \quad 0 \leq \ell < \frac{1}{2}, \tag{18}$$

$$\left.\begin{aligned} &\Psi_{2,0}(\ell) = \sqrt{2}, \\ &\Psi_{2,1}(\ell) = \sqrt{6}(2\ell - 1), \\ &\Psi_{2,2}(\ell) = \sqrt{\tfrac{30}{7}}\left(2\ell^2 - 2\ell + 1\right), \\ &\Psi_{2,3}(\ell) = \sqrt{\tfrac{480}{304}}\left(8\ell^3 - 12\ell^2 + 10\ell - 3\right), \end{aligned}\right\} \quad \frac{1}{2} \leq \ell < 1. \tag{19}$$

The FW representation allows for expressing any function $f \in L^2[0, 1)$ in terms:

$$f(\ell) \approx \sum_{\mathrm{m}=1}^{2^{k-1}} \sum_{\mathrm{n}=0}^{M-1} G_{\mathrm{m,n}} \Psi_{\mathrm{m,n}}(\ell), \tag{20}$$

where

$$G_{\mathrm{m,n}} = \left\langle f, \Psi_{\mathrm{m,n}} \right\rangle = \int_0^1 f(\ell) \Psi_{\mathrm{m,n}}(\ell) d\ell.$$

The coefficients of the FW correspond to the matrix representation of Eqs. (20), which can be expressed as follows:

$$f(\ell) = G^T \Psi(\ell). \tag{21}$$

The matrix $\Psi(\ell)$ in Eq. (21) represents a FW matrix and has an order of $1 \times 2^{k-1}M$. It can be written as:

$$\Psi(\ell) = \left[\Psi_{1,0}, \Psi_{1,1}, \dots, \Psi_{1,M-1}, \Psi_{2,0}, \Psi_{2,1}, \dots, \Psi_{2,M-1}, \dots, \Psi_{2^{k-1},0}, \Psi_{2^{k-1},1}, \dots, \Psi_{2^{k-1},M-1}\right]^T, \tag{22}$$

where $\Psi_{n,m}$ represents the entry at the nth row and mth column of the FW matrix. Similarly, the row vector G is defined as follows:

$$G = \left[G_{1,0}, G_{1,1}, \dots, G_{1,M-1}, G_{2,0}, G_{2,1}, \dots, G_{2,M-1}, \dots, G_{2^{k-1},0}, G_{2^{k-1},1}, \dots, G_{2^{k-1},M-1}\right]^T. \tag{23}$$

Finally, it is important to consider the collocation points, which provide the specific locations at which the function values are evaluated.

$$\ell_\mu = \frac{2\mu - 1}{2^k M}, \quad \mu = 1, 2, \dots, 2^{k-1}M. \tag{24}$$

OMFI of Fibonacci wavelets

Here, we focus on the construction of OMFI and their applications in solving fractional differential equations. Contrary to conventional orthogonal function-based operational matrix techniques, we exploit the unique properties of FW to construct a generalized OMFI [22,33,34]

Block pulse function

The BPF, defined on the interval $[0, 1)$, can be expressed as follows:

$$b_v(\ell) = \begin{cases} 1, & \text{if } v\eta \leq \ell < (\eta + 1)v, \\ 0, & \text{otherwise}, \end{cases} \tag{25}$$

where $v = \frac{1}{N}$ and N is a positive integer. The variable η takes values in the range $\eta = 0, \dots, N-1$. And $f(\ell)$, belonging to $L^2[0, 1)$, can be estimated using the block-pulse functions:

$$f(\ell) \simeq f_N(\ell) = \sum_{\eta=1}^{N-1} a_\eta b_\eta(\ell) = A^T S_N. \tag{26}$$

Here, $A = [a_0, a_1, a_2, \ldots, a_{N-1}]$ and $S_N = [S_0, S_1, S_2, \ldots, S_N]^T$. By integrating $S_N(\ell)$, we have:

$$\int_0^{\ell} S_N(x)dx \simeq \Delta S_N(\ell).$$

Thus, the operational matrix of integration for BPF can be derived as:

$$\Delta = \frac{q}{2}\begin{pmatrix} 1 & 2 & 2 & \ldots & 2 \\ 0 & 1 & 2 & \ldots & 2 \\ \vdots & \vdots & \vdots & \cdots & \vdots \\ 0 & 0 & 0 & \cdots & 1 \end{pmatrix}.$$

By utilizing BPF, the OMFI are obtained as:

$$\left(I^{\alpha} S_N\right)(\ell) \simeq F^{\alpha} S_N(\ell),$$

where

$$F^{\alpha} = \frac{1}{N^{\alpha}\Gamma(\alpha+2)}\begin{pmatrix} 1 & \ell_1 & \ell_2 & \ell_3 & \ldots & \ell_{N-1} \\ 0 & 1 & \ell_1 & \ell_2 & \ldots & \ell_{N-2} \\ 0 & 0 & 1 & \ell_1 & \ldots & \ell_{N-3} \\ \vdots & \vdots & \vdots & \vdots & \ldots & \vdots \\ 0 & 0 & \ldots & 0 & 1 & \ell_1 \\ 0 & 0 & 0 & \ldots & 0 & 1 \end{pmatrix}, \tag{27}$$

where, the ℓ_{η} 's in (27) have been defined as:

$$\ell_{\eta} = (\eta+1)^{\alpha+1} - 2\eta^{\alpha+1} + (\eta-1)^{\alpha+1}. \tag{28}$$

Fractional operational matrix of Fibonacci wavelet

By integrating Eq. (22), we have the approximation:

$$\int_0^{\ell} \Psi(x)dx \approx U\Psi(\ell). \tag{29}$$

Here, U represents the integration operational matrix for a FW of order $2^{k-1}M \times 2^{k-1}M$. Utilizing BPFs to represent the FW we have:

$$\Psi(\ell) = \Psi_{\mathrm{m,n}} S_N(\ell). \tag{30}$$

To find OMFI of order α we define:

$$D^{\alpha}\Psi(\ell) = U^{\alpha}_{\mathrm{m,n}}\Psi(\ell). \tag{31}$$

Here, the matrix $U^{\alpha}_{\mathrm{m,n}}$ embodies OMFI for FW. By taking Eqs. (30), and (31), we have

$$\left(D^{\alpha}\Psi\right)(\ell) \approx \left(D^{\alpha}\Psi_{\mathrm{m,n}} S_N\right)(\ell) = \Psi_{\mathrm{m,n}}\left(D^{\alpha} S_N\right)(\ell) \approx \Psi_{\mathrm{m,n}} F^{\alpha} S_N(\ell). \tag{32}$$

Therefore, from (31) and (32), we get the following:

$$U^{\alpha}_{\mathrm{m,n}}\Psi(\ell) = U^{\alpha}_{\mathrm{m,n}}\Psi_{\mathrm{m,n}} S_N(\ell) = \Psi_{\mathrm{m,n}} F^{\alpha} S_N(\ell).$$

This leads to the derivation of the required OMFI of FW for arbitrary order.

$$U^{\alpha}_{\mathrm{m,n}} = \Psi_{\mathrm{m,n}} F^{\alpha}\left[\Psi_{\mathrm{m,n}}\right]^{-1}.$$

Specifically, when considering $k = 2$, $M = 3$, and $\alpha = 0.7$, we calculate the OMFI $U^{0.7}_{6\times6}$ as follows:

$$U^{0.7}_{6\times6} = \begin{pmatrix} 0.2781 & 0.4872 & -0.3112 & 0.4426 & -0.2191 & 0.2527 \\ -0.5224 & 0.0947 & 0.7290 & 0.3752 & -0.2523 & 0.3088 \\ -0.0845 & 0.3015 & 0.1813 & 0.4247 & -0.2405 & 0.2857 \\ 0 & 0 & 0 & 0.2781 & 0.4872 & -0.3112 \\ 0 & 0 & 0 & -0.5224 & 0.0947 & 0.7290 \\ 0 & 0 & 0 & -0.0845 & 0.3015 & 0.1813 \end{pmatrix}.$$

Error estimation and numerical results

Here, we discuss theorems on convergence analysis and study the estimation of error for Fibonacci wavelets method.

Theorem 1 ([18]). *Assume that $\Phi \in C^M[0,1)$ and $W_M = span\{\Psi_0(\ell), \Psi_1(\ell), \ldots, \Psi_{M-1}(\ell)\}$. If $\Phi_M(\ell) = H^T\hat{F}(\ell)$ represents the best approximation of $\Phi(\ell)$ from W_M over the interval $[\frac{u-1}{2^{k-1}}, \frac{u}{2^{k-1}}]$, the error bound for the approximate solution $\Phi^*(\ell)$ by FW on $[0,1)$ can be expressed as:*

$$\|E(\ell)\|_2 = \left\|\Phi - \Phi^*\right\|_2 \le \frac{R}{M!\sqrt{2M+1}}.$$

Theorem 2 ([33]). *Suppose that $\phi(\ell)$ is a smooth function defined on [0,1) and is square integrable. If $\phi(\ell)$ is bounded by a constant K, then it is possible to express $\phi(\ell)$ as a summation of Fibonacci wavelet. Furthermore, this series convergence to $\phi(\ell)$ uniformly, ensuring that the approximation becomes increasingly accurate for all values of ℓ in the interval [0,1). i.e,*

$$\phi(\ell) = \sum_{\mathrm{m}=1}^{2^{k-1}}\sum_{\mathrm{n}=0}^{M-1} \phi_{\mathrm{m,n}}\Psi_{\mathrm{m,n}}(\ell),$$

where

$$g_{\mathrm{m,n}} = \left\langle \phi(\ell), \Psi_{\mathrm{m,n}}(\ell)\right\rangle.$$

The precision of the Fibonacci wavelets collocation method is measured by the absolute error L_2 and maximum absolute errors L_{∞} by using the formulas given as

$$L_2 = \|\mu(\ell) - \mu^*(\ell)\|,$$

$$L_{\infty} = max|\mu(\ell) - \mu^*(\ell)|,$$

where $\mu(\ell)$ and $\mu^*(\ell)$ are the exact and approximate solutions respectively. The whole computational work is done on (Matlab–R2022a).

Numerical simulation

The approximation of fractional derivatives can be computationally challenging when modeling circuits of fractional order, which is crucial to recognize. Since accuracy and computing efficiency must coexist, a balance between the two should be sought in the numerical techniques used for simulation. Simulating these circuits involves solving the differential equations or difference equations that describe the behavior of the fractional order elements and analyzing the response of the circuit to different input signals. The goal of this section is to understand the unique dynamics and characteristics exhibited by fractional order circuits and study their impact on system performance and behavior. All the simulation and graphical results are obtain by using MatlabR2022a.

$\mathcal{LC}$ **Circuit:** The fractional order equation of an $\mathcal{LC}$ circuit represents a combination of a charged capacitor and an inductor. Assume that $\zeta = \sqrt{\frac{1}{\mathcal{LC}}}$ and $\mathcal{E}(\ell) = 0$, Eq. (3) becomes

$$D^{\alpha}[q(\ell)] + \zeta^2 q(\ell) = 0, \quad \alpha \in (1,2], \tag{33}$$

with ICs $q(0) = q_0$, and $D^{\alpha}[q(0)] = 0$. The exact solution for $\alpha = 2$ is

$$q(\ell) = q_0\cos(\zeta_0\ell).$$

To find the numerical solution of Eq. (33) by using FW, expressed the term containing fractional derivative as

$$D^{\alpha}[q(\ell)] = G_m^T\Psi_m(\ell). \tag{34}$$

Integrate (34) twice w.r.t ℓ, with order α we have

$$q(\ell) = G_m^T U^{\alpha}\Psi_m(\ell) + \ell D^{\alpha}[q(0)] + q(0).$$

Utilizing the ICs, we obtain

$$q(\ell) = G_m^T U^{\alpha}\Psi_m(\ell) + q_0. \tag{35}$$

Substituting Eqs. (34) and (35) in (33) we have

$$G_m^T\Psi_m(\ell) + \zeta^2[G_m^T U^{\alpha}\Psi_m(\ell) + q_0] = 0. \tag{36}$$

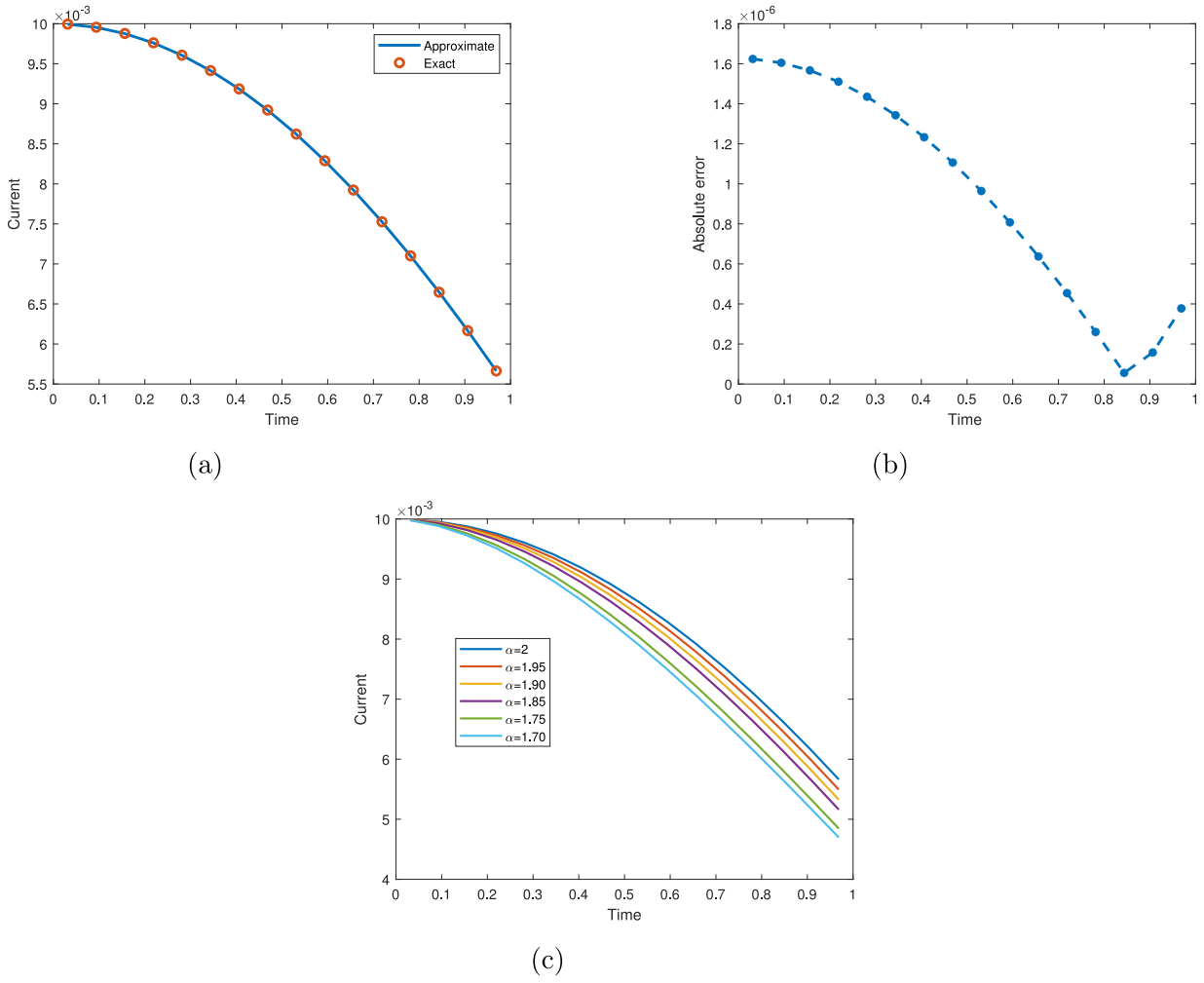

Fig. 1. (a) Comparison of exact and approximate solution (b) Absolute error (c) Behavior of approximate solution at different value of fractional parameter α.

Table 1
Absolute error of $\mathcal{LC}$ at $\alpha = 2$.

ℓ	Exact	FWM	Absolute error
0.1	0.009995	0.009993	1.6238e−06
0.2	0.009878	0.009876	1.5668e−06
0.3	0.009761	0.009760	1.5102e−06
0.4	0.009414	0.009413	1.3426e−06
0.5	0.008921	0.008920	1.1063e−06
0.6	0.008288	0.008287	8.0752e−07
0.7	0.007526	0.007525	4.5413e−07
0.8	0.006646	0.006646	5.5483e−08
0.9	0.006167	0.006167	1.5751e−07

This is the system of algebraic equations. Solving this system using Newton method yields the unknown coefficients. After substituting the coefficients into Eq. (35), we obtain the approximate solution. The numerical simulation was carried out for $\mathcal{L} = 1$, $C = 1$, and $q_0 = 0.01$. Fig. 1(a) depicts the comparison between the exact and approximate solutions at $\alpha = 2$. In Fig. 1(b), the absolute error is shown graphically. Fig. 1(c) illustrates the behavior of the numerical solution at various values of the fractional parameter $\alpha = 2, 1.95, 1.90, 1.85, 1.75, 1.70$ for the $\mathcal{LC}$ circuit. Table 1, presents the exact and approximate solutions, and absolute error at $\alpha = 2$ for a resolution of $k = 2$ and $M = 3$. After calculating the absolute error of an $\mathcal{LC}$ circuit, at each time step, we measure the difference between the two solutions.

$\mathcal{RC}$ circuit: Consider the fractional $\mathcal{RC}$ circuit with resistance and a charged capacitor. Let $\mu = \frac{1}{\mathcal{RC}}$ and $\mathcal{E}(\ell) = 0$. The associated fractional order differential equation (5) becomes

$$D^{\alpha}[q(\ell)] + \mu q(\ell) = 0, \quad \text{where } 0 < \alpha \leq 1 \tag{37}$$

with IC $q(0) = q_0$. The exact solution of (37) for $\alpha = 1$ is

$$q(\ell) = q_0 e^{-\mu \ell}.$$

To find the approximate solution we expanding the fractional derivatives in (37) using FW as

$$D^{\alpha}[q(\ell)] = G_m^T \Psi_m(\ell). \tag{38}$$

Integrate Eq. (38) w.r.t. ℓ, we obtain

$$q(\ell) = G_m^T U^{\alpha} \Psi_m(\ell) + q(0).$$

Utilizing ICs we have

$$q(\ell) = G_m^T U^{\alpha} \Psi_m + q_0. \tag{39}$$

Substituting Eqs. (38), (39) into Eq. (37) we have

$$G_m^T \Psi_m + \mu [G_m^T U^{\alpha} \Psi_m + q_0] = 0.$$

The above equation is solved by using Newton method to find the wavelet coefficients vector G_m^T. After substituting the coefficient in Eq. (39) we obtain the approximate solution.

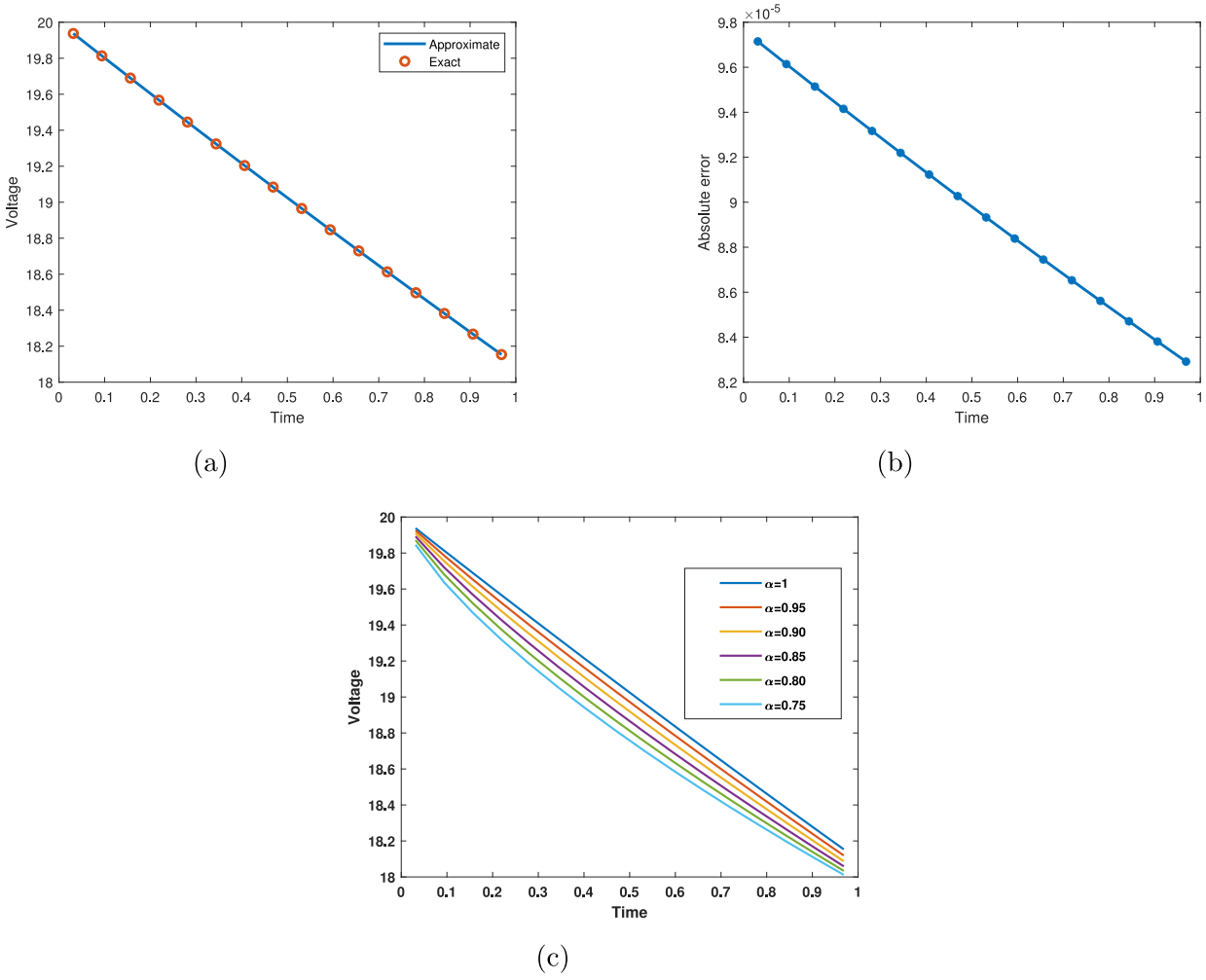

Fig. 2. (a) Comparison of exact and approximate solution (b) Absolute error (c) Behavior of approximate solution at different value of fractional parameter α.

Table 2
Absolute error at $\alpha = 1$.

ℓ	Exact	FWM	Absolute error
0.1	19.937597	19.937694	9.7149e−05
0.2	19.689928	19.690023	9.5141e−05
0.3	19.445336	19.445429	9.3168e−05
0.4	19.203782	19.203873	9.1230e−05
0.5	18.965229	18.965318	8.9325e−05
0.6	18.847066	19.847154	8.8385e−05
0.7	18.612944	18.613030	8.6529e−05
0.8	18.381730	18.381815	8.4706e−05
0.9	18.267203	18.267286	8.3807e−05

The numerical results are obtain for $\mathcal{R} = 10$ $C = 1$ with $q_0 = 20$ at $\alpha = 1$, with resolution $k = 3$ and $M = 4$. Table 2 shows the numerical solutions for the $\mathcal{R}C$ circuit when $\alpha = 1$. Fig. 2 provides graphical representations of the exact and approximate solutions, as well as the behavior of the approximate solution for various values of $\alpha = 1.0, 0.95, 0.90, 0.85, 0.80, 0.75$, while maintaining a resolution level of $k = 3$ and $M = 4$, along with the absolute error. The figures clearly demonstrate that when $\alpha = 1.0$ and $k = 2$, $M = 3$, the behavior of the fractional $\mathcal{R}C$ circuit closely resembles with the exact solution.

$\mathcal{RL}$ circuit: The $\mathcal{RL}$ circuit is an important component in many electronic systems and is used in various applications, including filters, oscillators, and power supplies. The $\mathcal{RL}$ fractional circuit equation (7) for $\kappa = \frac{\mathcal{R}}{\mathcal{L}}$ and $\rho = \frac{E}{\mathcal{L}}$ becomes

$$D^{\alpha}[q(\ell)] + \kappa q(\ell) = \rho, \qquad 0 < \alpha \leq 1, \tag{40}$$

with ICs $q(0) = q_0$.

The exact solution is $q(\ell) = [q_0 - \frac{E\mathcal{L}}{\mathcal{R}}]e^{-\kappa\ell} + \frac{E\mathcal{L}}{\mathcal{R}}$.

Expanding the fractional derivatives in (40) using FW we have

$$D^{\alpha}[q(\ell)] = G_m^T \Psi_m(\ell). \tag{41}$$

Integrate Eq. (41) w.r.t. ℓ, we obtain

$$q(\ell) = G_m^T U^{\alpha} \Psi_m(\ell) + q(0).$$

Utilizing ICs we have

$$q(t) = G_m^T U^{\alpha} \Psi_m + q_0. \tag{42}$$

Substituting Eqs. (41), (42) into Eq. (40) we have

$$G_m^T \Psi_m + \kappa[G_m^T U^{\alpha} \Psi_m + q_0] = \rho. \tag{43}$$

The system of Eq. (43) can be solved using Newton method to find the wavelet coefficients vector G_m^T. After substituting the coefficient in Eq. (42) we obtain the approximate solution (see Fig. 3).

The numerical simulation was carried out at $\mathcal{R} = 10$ $\mathcal{L} = 1$, $q_0 = 10$ at $\alpha = 1$. Table 3 provides the numerical solutions for the $\mathcal{RL}$

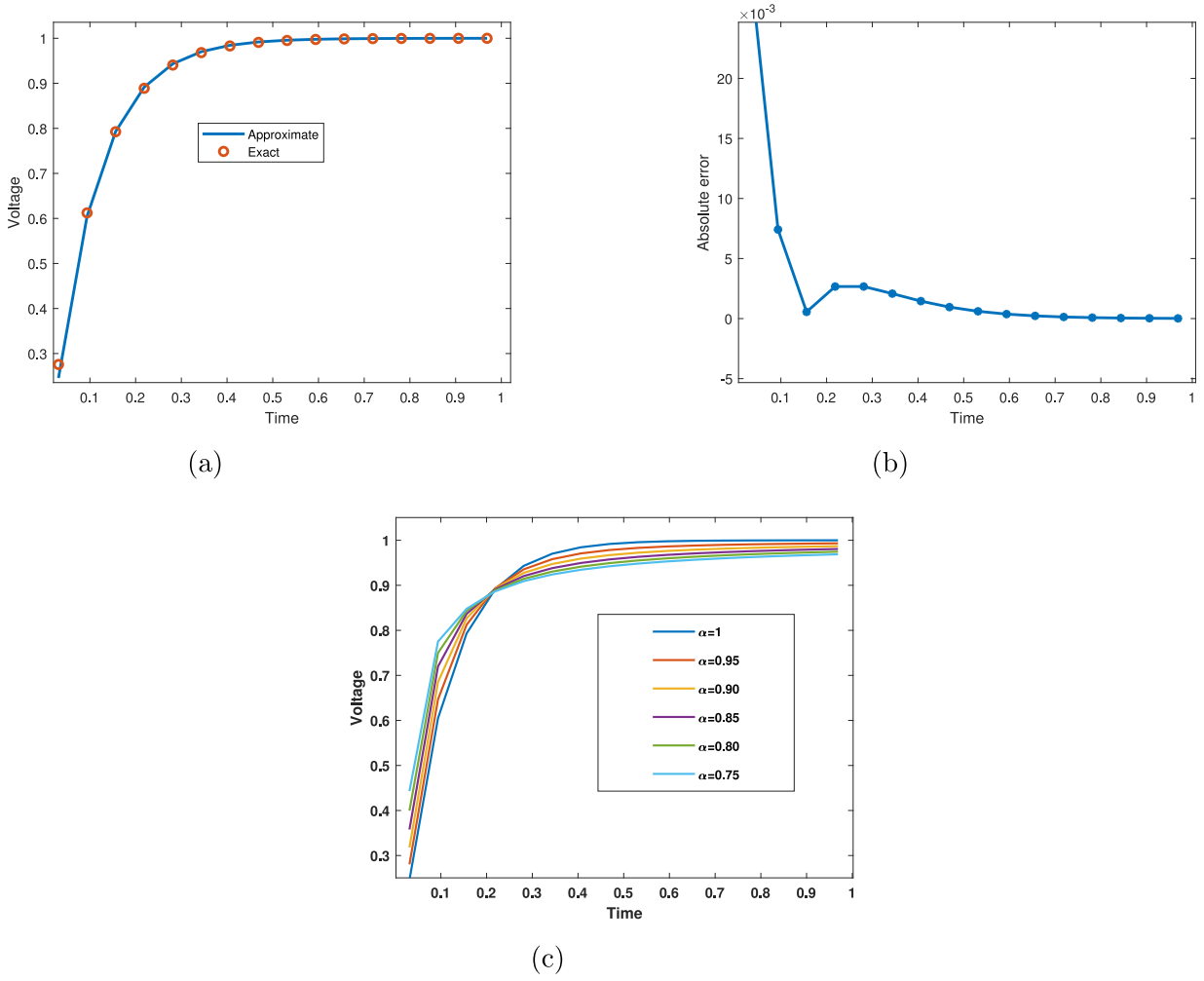

Fig. 3. (a) Comparison of exact and approximate solution (b) Absolute error (c) Behavior of approximate solution at different value of fractional parameter α.

Table 3
Absolute error of $\mathcal{RL}$ at various values of $\alpha = 1$.

ℓ	Exact	FWM	Absolute error
0.1	0.275700	0.275241	4.5900e−04
0.2	0.792484	0.793041	5.5706e−04
0.3	0.940545	0.940263	2.8200e−04
0.4	0.998601	0.998827	2.2530e−04
0.5	0.999251	0.999385	1.3403e−04
0.6	0.999599	0.999678	7.8776e−05
0.7	0.999785	0.999831	4.5851e−05
0.8	0.999885	0.999911	2.6473e−05
0.9	0.999938	0.999953	1.5181e−05

circuit at $\alpha = 1$ with resolution level $k = 3$ and $M = 4$ of Fibonacci wavelet. Additionally, Fig. 2 presents graphical analysis of exact and approximate solutions and behavior of numerical solution for various values of $\alpha = 1.0, 0.95, 0.90, 0.85, 0.80, 0.75$, while keeping $k = 2$ and $M = 3$ resolution level. It is evident from the figures that when $\alpha = 1$ and $k = 2, M = 3$, the behavior of the fractional $\mathcal{RL}$ circuit closely resembles the exact solution.

$\mathcal{RLC}$ circuit The dynamics of a fractional $\mathcal{RLC}$ circuit are governed by fractional order differential equations (9). Consider the fractional $\mathcal{RLC}$ circuit with resistance, inductance, and charged capacitance of $\mathcal{RLC}$ circuit for $\gamma = 2\alpha$, $\delta = \alpha$, $\beta = \mathcal{R}/\mathcal{L}$, $\kappa = 1/\mathcal{LC}$, and $\mathcal{E}(\ell) = 0$ we have:

$$D^{(2\alpha)}[q(\ell)] + \beta D[q^{\alpha}(\ell)] + \kappa q(\ell) = 0, \quad \text{where } 0 \le \alpha \le 1, \tag{44}$$

with ICs $q(0) = q_0$ and $D^{\alpha}[q(0)] = 0$. The exact solution at $\alpha = 1$ is

$$q(\ell) = q_0 e^{-\beta\ell/2} \cos\left(\sqrt{k - \frac{\beta^2}{4}}\ell\right).$$

Applying FW to expand the term with highest derivatives as:

$$D^{2\alpha}[q(\ell)] = G_m^T \Psi_m. \tag{45}$$

Integrate Eq. (45) w.r.t ℓ, we have

$$D^{\alpha}[q(\ell)] = G_m^T U^{\alpha} \Psi_m + q^{\alpha}(0). \tag{46}$$

Again integrate Eq. (46) w.r.t ℓ, we obtain

$$q(\ell) = G_m^T U^{2\alpha} \Psi_m + \ell q^{\alpha}(0) + q(0). \tag{47}$$

Utilizing ICs equation (47) becomes

$$q(\ell) = G_m^T U^{2\alpha} \Psi_m + q_0. \tag{48}$$

Substituting Eqs. (45), (46) and (48) in Eq. (44) we have system of algebraic equation as

$$G_m^T \Psi_m + \beta[G_m^T U^{\alpha} \Psi_m] + \kappa[G_m^T U^{2\alpha} \Psi_m + q_0] = 0. \tag{49}$$

Solving the system (49) for FW coefficient G and after substituting the coefficient in Eq. (47) we have the approximate solution.

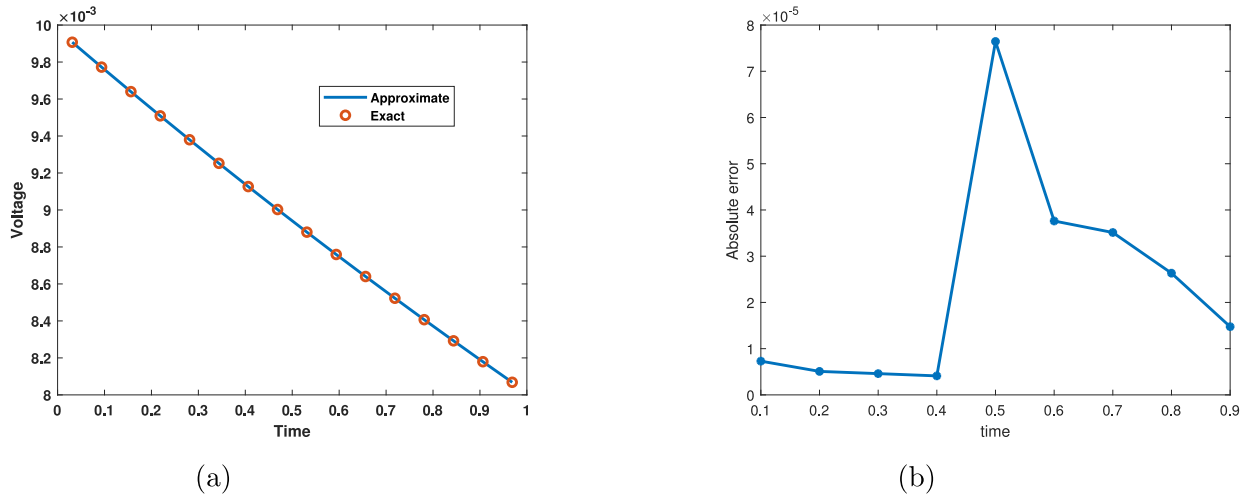

Fig. 4. (a) Comparison of exact and approximate solution (b) Absolute error at $\alpha = 1$.

Table 4
CPU time of $\mathcal{LC}, \mathcal{RC}, \mathcal{RL}$, and $\mathcal{RLC}$ circuits at k = 3, M = 4.

	$\mathcal{LC}$	$\mathcal{RC}$	$\mathcal{RL}$	$\mathcal{RLC}$
CPU time (s)	0.324	0.336	0.362	0.314

Fig. 4, shows the comparison of FW solutions with exact solution of $\mathcal{RLC}$ fractional model at resolution level $k = 2, M = 4$ for $\alpha = 1$. Also we plotted the graph of absolute error at $\alpha = 1$ depicts that the FW method give more precise solutions for these models.

In Table 4, we have shown the computation time for $\mathcal{LC}, \mathcal{RC}, \mathcal{RL}$, and $\mathcal{RLC}$ circuits at resolution level k = 3, M = 4 of FWM.

Conclusion

We have developed an effective numerical method based on FW for solving fractional order ECs models such as $\mathcal{LC}, \mathcal{RC}, \mathcal{RL}$, and $\mathcal{RLC}$. By constructing the operational matrices of integration of the FW, the simplification was achieved, and the problems were reduced to a sparse systems of linear equations, which are computed by Newton iteration method. Four cases of ECs at different values of the parameters are used to illustrate how well the FW collocation approach works. The outcomes are presented in the form of tables and figures and also compared with exact solutions. The absolute error is calculated to demonstrate the accuracy and efficiency of the approach. The findings indicate that the FW method offers improved accuracy and efficiency in analyzing and designing fractional order systems. Moreover, it successfully captures the intricate behavior of complex systems. The fractional parameter α significantly impacts the dynamics and control of fractional ECs, understanding and appropriately selecting the fractional order are vital for designing and analyzing such circuits in modern technology applications. Tables and figures presenting the numerical solutions allow us to see how well the FW solutions coincide with exact solutions. The findings of this study indicate that the combination of Caputo fractional derivatives and FW-based methods offers a reliable and robust numerical approach for investigating fractional order dynamics in ECs. This method offers physicists a strong and useful choice for effectively analysing these kinds of differential equations and can be applied to similar physics problems.

CRediT authorship contribution statement

Shahid Ahmed: Writing – original draft, Writing – review & editing, Conceptualization, Data curation, Formal analysis, Methodology, Validation, Visualization, Revise the manuscript. **Kamal Shah:** Writing – original draft, Writing – review & editing, Conceptualization, Data curation, Formal analysis, Methodology, Validation, Visualization, Revise the manuscript. **Shah Jahan:** Writing – original draft, Writing – review & editing, Conceptualization, Data curation, Formal analysis, Methodology, Supervision, Validation, Visualization, Revise the manuscript. **Thabet Abdeljawad:** Writing – original draft, Writing – review & editing, Conceptualization, Data curation, Formal analysis, Methodology, Validation, Visualization, Revise the manuscript.

Declaration of competing interest

The authors declare that they have no known competing financial interests or personal relationships that could have appeared to influence the work reported in this paper.

Data availability

No data was used for the research described in the article

Acknowledgments

Authors Kamal Shah and Thabet Abdeljawad are thankful to Prince Sultan University, Saudi Arabia for paying the APC and support through TAS research lab. We would also like to thank Central University of Haryana for providing necessary facilities to carry out this research.

References

[1] Podlubny I. Fractional differential equations: an introduction to fractional derivatives fractional differential equations, to methods of their solution and some of their applications. Elsevier; 1998.
[2] Miller KS, Ross B. An introduction to the fractional calculus and fractional differential equations. New York: Wiley; 1993.
[3] Khan H, Alzabut J, Gulzar H, Tunç O, Pinelas S. On system of variable order nonlinear p-Laplacian fractional differential equations with biological application. Mathematics 2023;11(8):1913.
[4] Khan H, Alzabut J, Shah A, He ZY, Etemad S, Rezapour S, Zada A. On fractal-fractional waterborne disease model: A study on theoretical and numerical aspects of solutions via simulations. Fractals 2023;2340055.

[5] Diethelm K, Neville JF. Analysis of fractional differential equations. J Math Anal 2002;265(2):229–48.
[6] Gómez JF, Astorga CM, Escobar RF, Medina MA, Guzmán R, Gonzáleg A, Baleanu D. Overview of simulation of fractional differential equation using numerical Laplace transform. Cent Eur J Phys (CEJP) 2015;1–14.
[7] Atangana A, Nieto JJ. Numerical solution for the model of RLC circuit via the fractional derivative without singular kernel. Adv Mech Eng 2015;7(10):1687814015613758.
[8] Al-Zhour Z. Fundamental fractional exponential matrix new computational formulae and electrical applications. Int J Electron Commun 2021;129:153557.
[9] Khan H, Alzabut J, Shah A, Etemad S, Rezapour S, Park C. A study on the fractal-fractional tobacco smoking model. AIMS Math 2022;7(8):13887–909.
[10] Alzabut J, Selvam AGM, El-Nabulsi RA, Dhakshinamoorthy V, Samei ME. Asymptotic stability of nonlinear discrete fractional pantograph equations with non-local initial conditions. Symmetry 2021;13(3):473.
[11] Arora R, Chauhan NS. An application of Legendre wavelet in fractional electrical circuits. Glob J Pure Appl Math 2017;13(2):183–202.
[12] Shah PV, Patel AD, Salehbhai IA, Shukla AK. Analytic solution for the electric circuit model in fractional order. In: Abstr Appl Anal. Hindawi; 2014.
[13] Gill V, Modi K, Singh Y. Analytic solutions of fractional differential equation associated with RLC electrical circuit. Int J Stat Manag Syst 2018;21(4):575–82.
[14] Alsaedi A, Nieto JJ, Venktesh V. Fractional electrical circuits. Adv Mech Eng 2015;7(11).
[15] Gómez-Aguilar JF, Yépez-Martínez H, Escobar-Jiménez RF, Astorga-Zaragoza CM, Reyes-Reyes J. Analytical and numerical solutions of electrical circuits described by fractional derivatives. Appl Math Model 2016;40(21–22):9079–94.
[16] Sene N, Gómez-Aguilar JF. Analytical solutions of electrical circuits considering certain generalized fractional derivatives. Eur Phys J Plus 2019;134(6):260.
[17] Chen CF, Hsiao CH. Haar wavelet method for solving lumped and distributed-parameter systems. IEE Proc Control Theory Appl 1997;144(1):87–94.
[18] Yadav P, Jahan S, Nisar KS. Fibonacci wavelet collocation method for fredholm integral equations of second kind. Qual Theory Dyn Syst 2023;22(2):82.
[19] Shah FA, Irfan I, Nisar KS. Gegenbauer wavelet quasi-linearization method for solving fractional population growth model in a closed system. Math Methods Appl Sci 2022;45(7):3605–23.
[20] Hussain B, Afroz A, Jahan S. Approximate solution for proportional delay Reccati differential equations by Haar wavelet method. Poincare J Anal 2021;8(2):155–68.
[21] Ahmed S, Jahan S, Nisar KS. Hybird Fibonacci wavelet method to solve fractional-order logistic growth model. Math Methods Appl Sci 2023;1–14.
[22] Yadav P, Jahan S, Nisar KS. Solving fractional Bagley–Torvik equation by fractional order Fibonacci wavelet arising in fluid mechanics. AIN Shams Eng J 2023;102299.
[23] Altaf S, Khan YS. Numerical solution of fractional electrical circuits by haar wavelet. Matematika 2019;35.
[24] Chauhan NS. A new approach for solving fractional RL circuit model through quadratic Legendre multi-wavelets. J Math Phys 2018;1(1).
[25] Adel M, Srivastava HM, Khader MM. Implementation of an accurate method for the analysis and simulation of electrical RL circuits. Math Methods Appl Sci 2023;46(7):8362–71.
[26] Mirzaee F, Hoseini SF. Application of Fibonacci collocation method for solving Volterra-Fredholm integral equations. Appl Math Comput 2016;273:637–44.
[27] Mirzaee F, Hoseini SF. Numerical approach for solving nonlinear stochastic Itô-Volterra integral equations using Fibonacci operational matrices. Sci Iran 2015;22(6):2472–81.
[28] Mirzaee F, Hoseini SF. Solving systems of linear Fredholm integro-differential equations with Fibonacci polynomials. AIN Shams Eng J 2014;5(1):271–83.
[29] Mirzaee F, Hoseini SF. Solving singularly perturbed differential-difference equations arising in science and engineering with Fibonacci polynomials. Results Phys 2013;3:134–41.
[30] Mirzaee F, Hoseini SF. A new collocation approach for solving systems of high-order linear Volterra integro-differential equations with variable coefficients. Appl Math Comput 2017;311:272–82.
[31] Gómez-Aguilar JF. Fundamental solutions to electrical circuits of non-integer order via fractional derivatives with and without singular kernels. Eur Phys J Plus 2018;133:197.
[32] Sun H, Zhang Y, Baleanu D, Chen W, Chen Y. A new collection of real world applications of fractional calculus in science and engineering. Commun Nonlinear Sci Numer Simul 2018;64:213–31.
[33] Shah FA, Irfan I, Nisar KS, Matoog RT. Fibonacci wavelet method for solving time-fractional telegraph equations with Dirichlet boundary conditions. Results Phys 2021;24:104123.
[34] Atangana A, Nieto JJ. Numerical solution for the model of RLC circuit via the fractional derivative without singular kernel. Adv Mech Eng 2015;7(10):1687814015613758.